Implication of extreme atmospheric methane concentrations for chemistry-climate connections

Franziska Winterstein[1], Fabian Tanalski[1,2], Patrick Jöckel[1], Martin Dameris[1], and Michael Ponater[1]

[1]Deutsches Zentrum für Luft- und Raumfahrt (DLR), Institut für Physik der Atmosphäre, Oberpfaffenhofen, Germany
[2]now at MERPH-IP Patentanwälte PartG mbB, München, Germany

Correspondence to: Franziska Winterstein (franziska.frank@dlr.de)

Abstract. Methane (CH_4) is the second most important greenhouse gas, which atmospheric concentration is influenced by human activities. In this study, numerical simulations with a chemistry-climate model (CCM) are performed aiming to assess possible consequences of significantly enhanced CH_4 concentrations in the Earth's atmosphere for the climate.

We analyze experiments with $2xCH_4$ and $5xCH_4$ present day (2010) mixing ratio and its quasi-instantaneous chemical im-
5 pact on the atmosphere. The massive increase in CH_4 strongly influences the tropospheric chemistry by reducing the hydroxyl radical (OH) abundance and thereby extending the CH_4 lifetime as well as the residence time of other chemical pollutants. The region above the tropopause is impacted by a substantial rise in stratospheric water vapor (SWV). The stratospheric ozone (O_3) column increases overall, but SWV induced stratospheric cooling also leads to a enhanced ozone depletion in the Antarctic lower stratosphere. Regional patterns of ozone change are affected by modification of stratospheric dynamics, i.e. increased
10 tropical up-welling and stronger meridional transport towards the polar regions. We calculate the net radiative impact (RI) of the $2xCH_4$ experiment to be 0.69 W/m^2 and for the $5xCH_4$ experiment to be 1.79 W/m^2. A substantial part of the RI is contributed by chemically induced O_3 and SWV changes, in line with previous radiative forcing estimates.

To our knowledge this is the first numerical study using a CCM with respect to two/fivefold CH_4 concentrations and it is therefore an overdue analysis as it emphasizes the impact of possible strong future CH_4 emissions on atmospheric chemistry
15 and its feedback on climate.

1 Introduction

Methane (CH_4) is a potent greenhouse gas (GHG), subject to strong anthropogenic emissions that contribute substantially to global warming. It is not just by itself a radiatively active gas but is chemically active as well, strongly influencing the chemical composition of the atmosphere. Beyond that its sources are prone to temperature and it is generally expected that
20 climate change (i.e. surface warming) will lead to enhanced CH_4 emissions, accelerating the temperature rise. For instance additional CH_4 emissions are expected from wetlands due to climate-driven changes (Gedney et al., 2004; Zhang et al., 2017; Ma et al., 2017). Moreover, a large quantity of CH_4 is stored as methane hydrate not only in permafrost soil but also in the sea floor. Permafrost soil stores about a hundredfold of the current CH_4 burden in the atmosphere and oceanic methane hydrates

store even a thousandfold (IPCC, 2013). Current estimates indicate that GHG emissions from thawing permafrost soils could represent a major terrestrial biogeochemical feedback to climate change over the coming decades (Comyn-Platt et al., 2018).

At the same time, it is under debate whether a possible strong release of CH_4 from thawing permafrost in the Arctic region could potentially force an abrupt climate change (as discussed by O'Connor et al., 2010). At present, the release of methane hydrate from reservoirs is highly uncertain as well as the magnitude of future natural and anthropogenic emissions of methane.

5 Increasing surface temperatures cause enhanced CH_4 emissions from thawing permafrost soils to the atmosphere, but the amount is currently poorly constrained (Hayes et al., 2014; Schaefer et al., 2014; Koven et al., 2015; Schuur et al., 2015). For instance, Dean et al. (2018) stated that there is basically no significant increase of Arctic methane emissions at the moment, though it may increase towards the end of the 21st century.

Nevertheless, permafrost thaw could potentially release trapped CH_4 and transform frozen soil to wetland areas, which

10 would then add to Arctic CH_4 emissions. Moreover, ongoing heating of the Arctic sea surface temperature (SST) will also enhance future CH_4 production in the ocean , and a reduction of sea ice concentration (SIC) may increase the direct transfer of CH_4 from the ocean to the atmosphere. In particular, enhanced SST can increase the production of CH_4 as permafrost underlying the continental shelf begins to thaw (Miller et al., 2018). How a changing climate will impact future CH_4 emissions remains a topic of debate in atmospheric science, since emissions from the most climate sensitive CH_4 sources, i.e. wetlands,

15 are difficult to quantify precisely.

Although there remain important knowledge gaps about the magnitude of CH_4 emissions, it is important to improve our understanding of how strongly future CH_4 emissions may impact our atmosphere and the environment. About 90% of the emitted CH_4 is removed in the troposphere. A change in tropospheric CH_4 concentration affects the oxidizing capacity of the atmosphere, modifies ozone in the troposphere and influences the CH_4 lifetime itself (e.g. Saunois et al., 2016; Frank, 2018;

20 Holmes, 2018). Additionally, it also influences the stratosphere. For example, enhanced CH_4 emissions will lead to increased abundance of stratospheric water vapor (SWV) and by this strongly influence stratospheric ozone (O_3) (Stenke and Grewe, 2005; Revell et al., 2016).

To assess the direct and indirect effects of severely enhanced CH_4 emissions on atmospheric composition and Earth climate, numerical model studies are able to support investigations such as to identify potential signatures impacting climate change. So

25 far only a limited amount of numerical studies are available concerning the impact of very strong CH_4 emissions. Exemplary, the effect of twofold CH_4 was investigated in a 1D radiative-convective climate model by Owens et al. (1982) and by MacKay and Khalil (1991). Shang et al. (2015) used a Chemical Transport model (CTM) but doubled CH_4 emission over China only. Other CTM studies have focused on recent changes and fluctuations of the atmospheric CH_4 concentration (e.g. Dalsøren et al., 2016) or have tried to explain CH_4 trends, which is a challenge because of important uncertainties in the global CH_4 budget,

30 i.e. the balance of surface sources and atmospheric and surface sinks (Saunois et al., 2016). Furthermore, CTMs are limited in assessing climate change related issues, because they do not include the feedback between chemistry and dynamics. Smith et al. (2018) investigated the fast radiative feedbacks (adjustments) in a $3 \times CH_4$ simulation without considering the chemical feedback effects. This investigation includes only physical components of the atmosphere, like direct cloud, water vapor and

temperature adjustments, and the total radiative adjustment result in a value near zero. This example even more motivates an assessment of simulations that include chemically driven atmospheric adjustments to increases of CH_4.

To our knowledge studies using data derived from chemistry-climate model (CCM) simulations including extreme CH_4 emissions (i.e. beyond current and near-future amounts) are not available so far. A CCM is an atmospheric global circulation model that is interactively coupled to a detailed chemistry module. In contrast to CTMs, in CCMs the simulated concentrations of the radiatively active gases are used for the calculations of net heating rates. Changes in the abundance of these gases due to chemistry and advection influence heating rates and, consequently, variables describing atmospheric dynamics. This creates a dynamical-chemical coupling in which the chemistry influences the dynamics and vice versa. Since CH_4 influences other trace gases due to its oxidation products as well as the removal of hydroxyl radical (OH), a comprehensive chemistry module is necessary. In simulations with doubled carbon dioxide (CO_2), in contrast, the feedback on climate and chemistry is induced only by its radiative impact. Apart from accounting for the direct radiative impact of CH_4 the use of a CCM is strongly desired, since the atmospheric CH_4 chemical feedback is a key process for understanding the variations in atmospheric CH_4 and its effects on other chemical constituents of the atmosphere (Holmes, 2018).

The present work is the first study investigating atmospheric effects due to extreme CH_4 emissions with such a CCM. Idealized simulations of significantly enhanced CH_4 concentrations are performed, i.e. twofold ($2xCH_4$) and fivefold ($5xCH_4$) enhanced CH_4 concentrations compared to present day condition, allowing to assess possible future consequences for atmospheric composition considering chemical feedback processes. In a first step, which is described in this paper, we conducted CCM simulations without interactive ocean coupling, i.e. the surface conditions regarding SST and SIC are prescribed (suppressed surface temperature feedback). Equivalent to the work of Smith et al. (2018), the results can be interpreted as rapid adjustments to a sudden CH_4 enhancement before the ocean reacts to the perturbation, which would occur on a by far larger time scale.

In this study we will use the ECHAM/MESSy Atmospheric Chemistry (EMAC) CCM (Jöckel et al., 2016) assessing the range of atmospheric responses by abrupt increases of CH_4 concentrations. A short description of EMAC is given in Section 2 as well as an explanation of the simulation strategy. In Section 3 the reference simulation representing near-present day condition is briefly evaluated with observations (Subsect. 3.1) and a discussion of the impact of twofold and fivefold increased CH_4 concentrations in respective scenario simulations is presented in Subsect. 3.2. In the final Section 4 we draw some conclusions from our investigation and give a brief outline for follow-up investigations.

2 Description of the model and simulation strategy

We use the EMAC model in the version 2.52 (Jöckel et al., 2010) and operate it at a resolution of T42L90MA corresponding to a quadratic Gaussian grid of approx. 2.8° x 2.8° in latitude and longitude with 90 levels up to 0.01 hPa. More details on the Modular Earth Submodel System (MESSy) can be found in Jöckel et al. (2016).

We conducted one reference simulation (REF) and two sensitivity simulations (S1 and S2) as 20-year time slice simulations representing in general year 2010 conditions. Monthly SST and SIC are thereby repeatedly prescribed, representing a climato-

logical annual cycle of the years 2000–2009 based on global analyses of Rayner et al. (2003). An at least 10-year long spin-up simulation preceeding each simulation (likewise time slice) ensures quasi steady state conditions, but has been neglected in the evaluation. The spin-up started with initial conditions using a restart file representing the year 2010 of a reference simulation with so called specified dynamics (SD) of the Earth System Chemistry integrated Modelling (ESCiMo) project (Jöckel et al., 2016). To reduce the length of the spin up of the sensitivity simulations we started those using twofold and fivefold CH_4 mixing

5   ratios compared to the initialization of the reference, respectively.

     The lower boundary condition of CH_4 in the reference simulation, i.e. the CH_4 surface mixing ratio, is prescribed by Newtonian relaxation (i.e. nudged) following a zonal mean estimate from the National Oceanic and Atmospheric Administration/Earth System Research Laboratory (NOAA/ESRL) based on observations of CH_4 surface mixing ratios. These observations are provided by the Advanced Global Atmospheric Gases Experiment (AGAGE; http://agage.eas.gatech.edu) and Na-

10   tional Oceanic and Atmospheric Administration/Earth System Research Laboratory (NOAA/ESRL; http://www.esrl.noaa.gov). The mean surface mixing ratio is about 1.8 parts per million volume (ppmv). The two sensitivity simulations (S1 and S2) are carried out nudged at the surface to a twofold CH_4 surface mixing ratio (compared to the present day reference) being about 3.6 ppmv and a fivefold CH_4 surface mixing ratio being 9.0 ppmv, respectively. Although this does not correspond to an equivalent increase in the surface fluxes, it scales the surface mixing ratio directly to the intended value, as has been done in similar

15   studies (see Kirner et al., 2015; Forster et al., 2016; Smith et al., 2018). To put the chosen scaling factors in perspective, a surface mixing ratio of 3.6 ppmv (similar to the doubling above) will be reached according to the Representative Concentration Pathways (RCP) 8.5 scenario towards the end of the 21st century (Riahi et al., 2007). The RCP 8.5 is the so called baseline climate change scenario, which does not employ any climate mitigation target (Riahi et al., 2011). Other prescribed conditions (SST, SIC, CO_2 etc.) of the sensitivity simulations S1 and S2 are identical to REF. Particularly all other GHG concentrations

20   and online simulated emissions represent 2010 conditions.

     In the following, changes and feedbacks are assessed by comparing the reference simulation REF with S1 and S2, with focus on changes in the simulated chemically and radiatively active trace gases. To quantify the associated radiative impact (RI), the EMAC option for multiple radiation calls is employed (Dietmüller et al., 2016) in a separate additional simulation, which allows to estimate individual components of the total radiative impact. This simulation is run for one year (plus one year

25   spin-up) and uses climatological 20 year means of the species of interest, namely CH_4, O_3 and SWV. The results corresponding to one of the previously introduced experiments are indicated by the associated simulations name and a asterixs (i.e. REF*, S1* and S2*).

3   Discussion of results

3.1   Evaluation of the reference simulation

30   The reference simulation REF is set up to represent conditions comparable to the near-present atmospheric conditions in 2010. To ensure that this simulation is sufficiently realistic, the simulation results of CH_4 mixing ratio in the troposphere and the

stratosphere are compared to data derived from atmospheric observations indicated below. These observations are independent to the data sets used for the lower boundary condition, to ensure an objective evaluation.

For a detailed assessment of the performance of EMAC in general and how EMAC compares to observations (e.g. regarding temperature and ozone) we refer to Jöckel et al. (2016). This publication also includes an evaluation of transient simulations regarding CH_4 in the Upper Troposphere and Lower Stratosphere (UTLS) using measurements of the Civil Aircraft for the Regular Investigation of the atmosphere Based on an Instrument Container (CARIBIC) project, which indicates a good representation with relative differences of less than 5%.

In general, observed surface mixing ratios of CH_4 indicate a north-south gradient with larger CH_4 mixing ratios in the Northern Hemisphere (NH) mostly due to large wetland regions and anthropogenic sources on the northern continents. This north-south gradient is by design (nudging to observation based zonal mean surface mixing ratios) apparent in the simulation data as well. The simulated gradient of the model is compared to observations during a ship cruise of the research vessel *Polarstern* (Klappenbach et al., 2015, see Supplement Fig. S1). The simulation results reproduce the observed north-south gradient of the ship cruise qualitatively well, although an offset of about 0.055 ppmv exists. Note that the observations in the *Polarstern* were conducted in 2014, while the simulation represents 2010 conditions. Global CH_4 surface mixing ratios have risen between 2010 and 2014 by about 0.030 ppmv, which explains a large part of the offset.

Additionally, the average vertical CH_4 profile of the REF simulation is evaluated using balloon borne measurements from Röckmann et al. (2011). The CH_4 mixing ratio in the troposphere is approximately constant as a result of well-mixed tropospheric conditions. Above the tropopause the mixing ratio of CH_4 decreases with altitude. This vertical gradient apparent in the balloon borne observations is reasonably reproduced in REF (see Supplement Fig. S2).

Furthermore, a general comparison of zonally averaged CH_4 mixing ratio above the tropopause of REF is done with observations from the Michelson Interferometer for Passive Atmospheric Sounding (MIPAS) instrument mounted on the ENVISAT satellite (Fischer et al., 2008). The zonally averaged CH_4 MIPAS climatology (2002–2012) in Plieninger (2017) corresponds qualitatively and quantitatively to our simulation results in Figure 1a.

Our simulation represents the observed CH_4 mixing ratios in the stratosphere and mesosphere and also shows the apparent double bulge in the upper stratosphere with slightly higher values in the NH.

Overall, the agreement of the reference simulation results with observations turned out to be sufficient for the purpose of our intended study. In the next section we compare the reference simulation with the two sensitivity simulations, to present the general impact of strongly enhanced CH_4 concentrations.

3.2 Impact of twofold and fivefold increased CH_4 concentrations

In this sub-section we investigate the impact of twofold and fivefold surface CH_4 mixing ratio on the chemical composition of the atmosphere and analyze the new chemical equilibrium after a sufficient spin up.

Since SST and SIC are prescribed, any possible feedback on tropospheric temperature is largely suppressed in the present simulations. Therefore, in this study we are only considering rapidly evolving chemical feedback effects including respective radiative adjustments and temperature adjustments in the stratosphere.
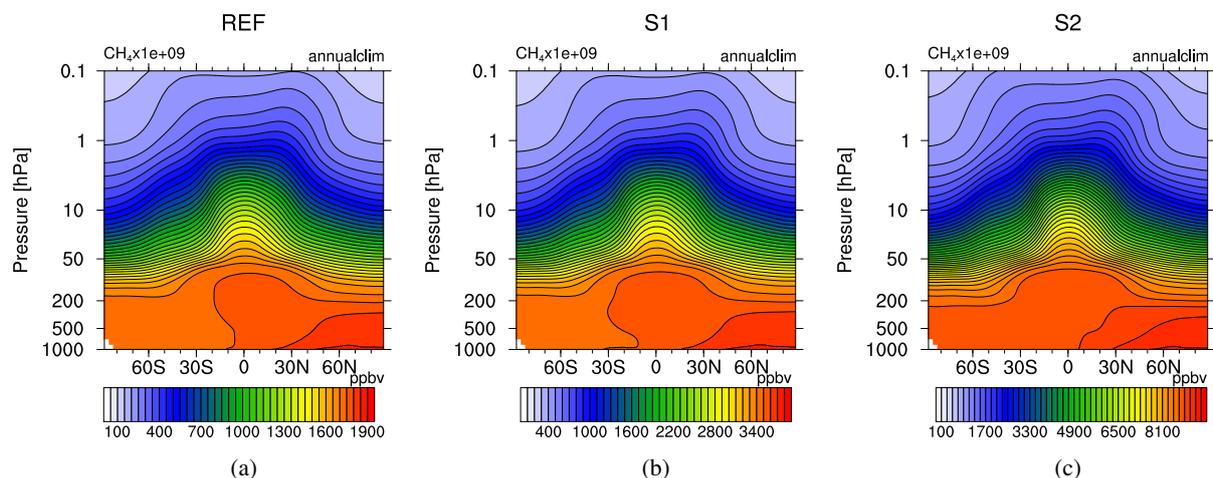
Figure 1. Annual zonal mean of absolute CH_4 mixing ratios (in parts per billion volume (ppbv)) of reference (REF) (a), S1 (b) and S2 (c). Note the different color scales.
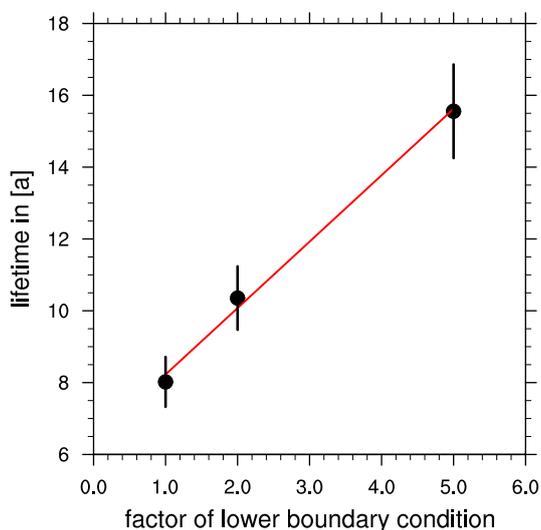
Figure 2. CH_4 lifetime calculated according to equation 1 versus the corresponding scaling factor applied to the reference lower boundary condition in the respective simulation: REF (1.0), S1 (2.0), S2 (5.0).

The oxidation capacity of the atmosphere is often measured in terms of the CH_4 lifetime (Karlsdóttir and Isaksen, 2000; Dentener et al., 2003; Naik et al., 2013; Voulgarakis et al., 2013). In this study we calculate the tropospheric CH_4 lifetime

15   according to Jöckel et al. (2006) as

$$\tau_{CH_4} = \frac{\sum_{b \in B} M_{CH_4}}{\sum_{b \in B} k_{CH_4+OH}(T) \cdot c_{air}(T,p,q) \cdot OH \cdot M_{CH_4}} \quad , \tag{1}$$
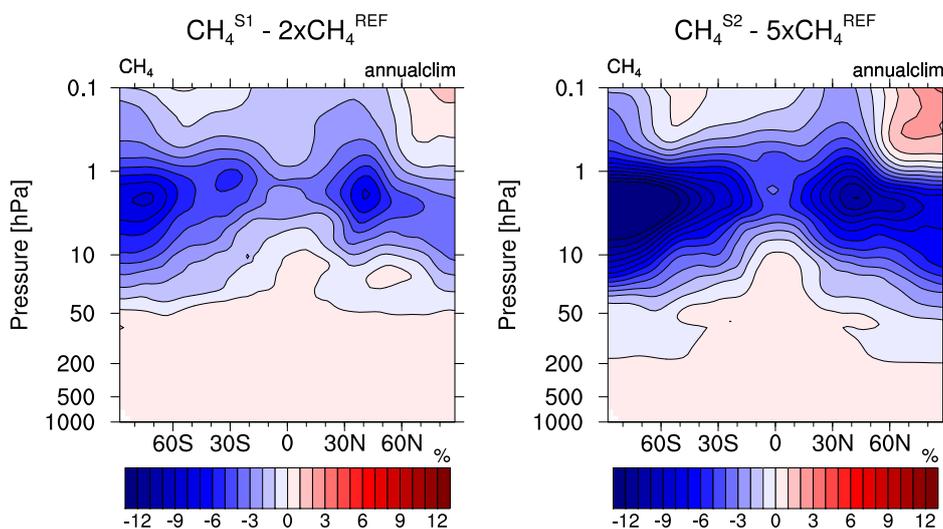
Figure 3. Difference between the annual zonal mean CH_4 of the simulations S1 relative to the twofold and S2 relative to the fivefold annual zonal mean of the reference in (%).

with M_{CH_4} being the mass of methane in kg, T the temperature, p the pressure and q the specific humidity, all depending on time and the specific box $b \in B$, with B being the set of all considered grid boxes, e.g. all boxes which lie below the tropopause. $k_{CH_4+OH}(T)$ is the reaction coefficient of the reaction $CH_4 + OH \longrightarrow$ products in [molec. s^{-1}]. $c_{air}(T,p,q)$ is the concentration of air in [molec. cm^{-3}] and OH the mole fraction of OH in one mole of the chemical tracer per one mole of air (mol mol^{-1})$_{dry\ air}$.

5   Our calculations yield a nearly linear increase of tropospheric CH_4 lifetime with respect to the CH_4 scaling in the sensitivity simulations (see Fig. 2). It is known that the tropospheric CH_4 lifetime is anti-correlated with OH concentration (Montzka et al., 2011). The strongly enhanced CH_4 mixing ratios reduce the atmospheric OH mixing ratio, which leads to a longer (tropospheric) CH_4 lifetime. It is not sure that the quasi-linear behavior will hold for even larger or smaller scaling factors, since the chemistry determining the OH abundance is highly non-linear. There are also not enough data points (sensitivity

10   simulations) for a definite proposition on strictly linear dependence. Nevertheless, we assume that these results give evidence that in the troposphere CH_4 and OH for the given range are almost linearly anti-correlated. The simulations clearly show that increasing CH_4 emissions increase the residence time of CH_4 in the atmosphere and therefore its global warming potential (GWP).

Next, we investigate the impact of CH_4 concentration increases on changes in CH_4 depletion, thus analyzing possible non-

15   linearities in the chemical cycles. For this we compare both sensitivity simulation results with the reference CH_4 mixing ratio multiplied by 2 and 5, respectively, as is shown in Fig. 3. This approach makes it possible to see where CH_4 is impacted by non-linear processes, hence where the twofolding (fivefolding) at the surface does not lead to an equal increase in the upper layers in the steady state.
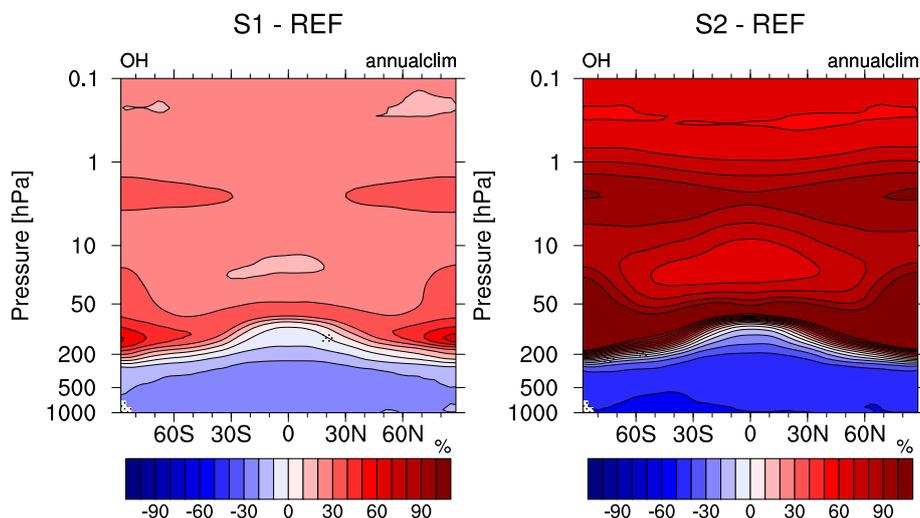
Figure 4. Comparison of the relative changes (%) in annual zonal mean OH mixing ratio of the sensitivity simulations S1 and S2 (two- and fivefold CH_4, respectively) compared to the reference REF. Non-stippled areas are significant on a 95% confidence level according to a two sided Welch's test.

In both sensitivity simulations, the troposphere is largely controlled by the nudging at the lower boundary due to turbulent mixing. In this area the differences of the sensitivity simulations and the scaled reference simulation are near-zero (though slightly positive). Larger CH_4 mixing ratios reduce its most important sink reactant in the troposphere, namely OH, which leads to a reduction of the CH_4 depletion compared to the reference.

The n-fold methane concentrations at the surface do not generate a likewise n-fold methane concentration throughout the
5 upper stratosphere. In the sensitivity simulation with twofold (fivefold) CH_4, lower CH_4 values of about 5% (10%) are found between 50 and 1 hPa compared to the corresponding n-folded reference. Identically prescribed SST in all three model simulations determines to a large extent the forcing of atmospheric dynamics and also constrains to a large part the stratosphere (see Garny, 2010). Therefore, modified atmospheric circulation patterns are unlikely the cause of these changes in stratospheric CH_4 mixing ratios.

10 An explanation for the relatively strong relative depletion in CH_4 in the upper stratosphere could be the change of the reaction rates for the CH_4 decomposition via OH and chlorine (Cl), which are both temperature dependent. However, since the stratosphere cools in the sensitivity simulations (as will be discussed below) this also cannot explain the simulated reduced CH_4 content in the stratosphere. Nevertheless, the deviation of a linear signal in stratospheric CH_4 mixing ratio gives evidence that more CH_4 in the upper stratosphere is destroyed due to secondary feedbacks caused by changes in the chemical composition
15 of the stratosphere (particular O_3, SWV and OH) and will be discussed in the paragraphs below.

The OH concentration in the atmosphere is determined by its precursors, which are water vapour (H_2O) and O_3, the photolysis rate of O_3, as well as by its sinks, which are mostly CH_4 and carbon monoxide (CO). The decline of OH in the troposphere
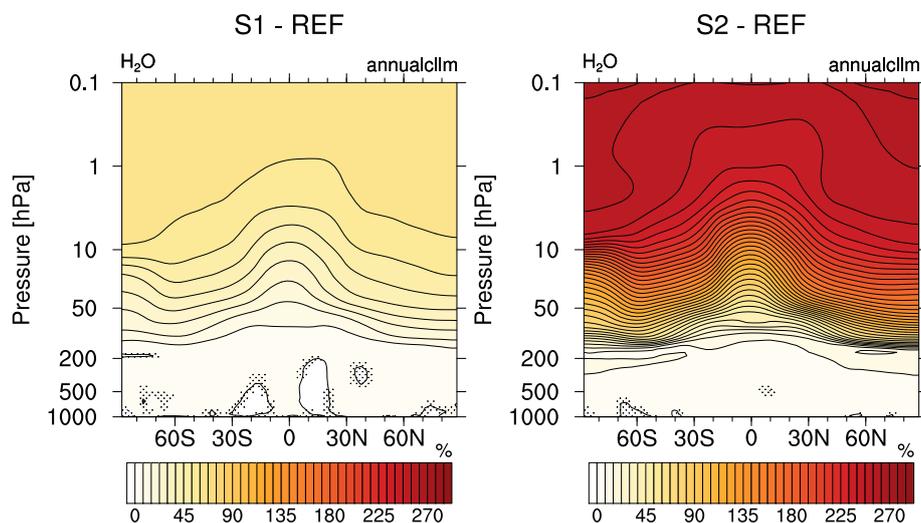
Figure 5. Comparison of the relative changes (%) in annual zonal mean H_2O mixing ratio of the sensitivity simulations S1 and S2 (two- and fivefold CH_4, respectively) compared to the reference REF. Non-stippled areas are significant on a 95% confidence level according to a two sided Welch's test.

by $20 - 30\%$ in the S1 simulation compared to REF (see Fig. 4) is caused, as stated above, by the increased sink via CH_4. In the stratosphere, however, OH increases by about 30% in the twofold CH_4 case (S1) and by $60 - 80\%$ in the fivefold CH_4 case (S2, see Fig. 4). The mixing ratio of OH increases especially in the upper stratosphere at higher latitudes and fits to the decline in CH_4 in the same regions (see Fig. 3). However, increases in CH_4 mixing ratios influence the abundance of OH precursors, namely H_2O and O_3 via direct and secondary chemical effects and thereby feedback on the production of the CH_4 associated

5 sink OH.

Oxidation of CH_4 in the stratosphere produces additional H_2O and is therefore an important source for SWV (Hein et al., 2001; Rohs et al., 2006; Frank et al., 2018). The enhanced CH_4 mixing ratios in the stratosphere cause a steady increase of SWV with height in both sensitivity simulations as indicated by Fig. 5. In the twofold CH_4 case (S1) the amount of H_2O is enhanced by up to 50% in the middle and higher stratosphere, in the fivefold experiment (S2) the SWV increases by more than

10 250%.

The chemical changes indicated above influence the atmospheric temperature. However, since the SST is prescribed, the temperature response is largely suppressed in the troposphere. Confirmation gives Fig. 6, where only a small change in tropospheric temperature is detected in both sensitivity simulations (S1 & S2). The stratosphere, however, shows larger changes in temperature. It can adjust to the perturbation since its temperature is mostly controlled by local radiative heating from trace

15 gases and changing dynamics.

Around the tropopause there is a slight warming in the twofold CH_4 case (S1), which is reaching values of up to $+3$ K in the fivefold case (S2, see Fig. 6). Elsewhere in the stratosphere, however, the higher abundance of CH_4 induces a stratospheric
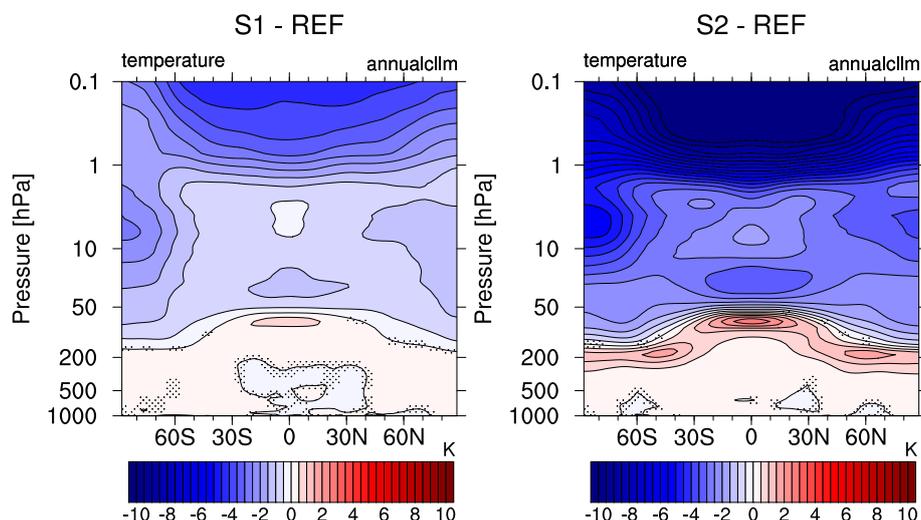
Figure 6. Comparison of the absolute changes (K) in annual zonal mean temperature of the sensitivity simulations S1 and S2 (two- and fivefold CH$_4$, respectively) compared to the reference REF. Non-stippled areas are significant on a 95% confidence level according to a two sided Welch's test.

cooling in our simulations. The twofold CH$_4$ mixing ratios in S1 lead to a stratospheric cooling of about $-1 - -2$ K and a mesospheric cooling of up to -5 K. The results of the simulation with fivefold CH$_4$ mixing ratios indicate a cooling of about -3 K in the stratosphere and more than -10 K in the mesosphere.

As will be shown below, these temperature changes are mainly induced by the radiative impact of CH$_4$ in the stratosphere
5   and mesosphere and by the changes in atmospheric chemistry due to enhanced chemically reactive CH$_4$.

Furthermore, the extreme CH$_4$ concentrations prescribed in our sensitivity simulations have an impact the vertical profile of O$_3$. Concentrations of O$_3$ increase between 50 and 5 hPa (see Fig. 7) and decrease above. There is also a decrease between 50 hPa and 20 hPa in the tropics and between 100 hPa and 50 hPa at the southern pole.

The pattern of ozone reduction in the lowermost tropical stratosphere is typical for an enhanced tropical up-welling, which
10   transports ozone depleted air from the upper troposphere to the lower stratosphere (Deckert and Dameris, 2008; Dietmüller et al., 2014). Although the main factor for such a strengthening, namely the SST, is prescribed, the increase in the GHG CH$_4$ alone can also lead to an enhanced tropical up-welling (Garny et al., 2011). A similar pattern in stratospheric ozone changes due to CH$_4$ increases (i.e. increase between 2000 and 2040–2049 according to the Intergovernmental Panel on Climate Change (IPCC) A1B greenhouse gas scenario) has been shown by Kirner et al. (2015). Nonetheless, we expect the impact on the
15   tropospheric up-welling to intensify further in simulations, where the SSTs can adjust to the CH$_4$ induced climate change.

In the middle stratosphere the O$_3$ production/depletion is influenced by the increased SWV and the corresponding stratospheric cooling, which restrains the reaction rates of O$_3$ depleting catalytic cycles (Portmann and Solomon, 2007; Braesicke et al., 2013). Furthermore, Excited oxygen (O(^{1}D)) is depleted by increased abundances of H$_2$O, which reduce the sink of O$_3$
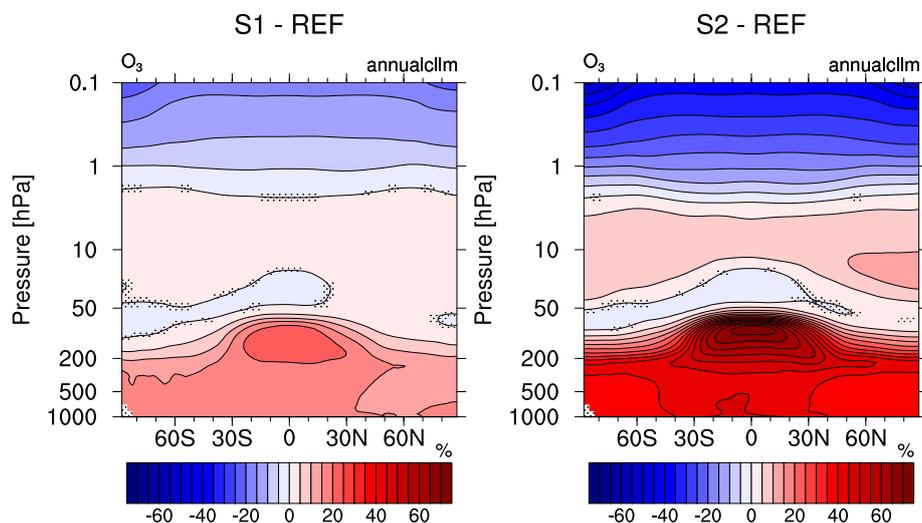
Figure 7. Comparison of the relative changes (%) in annual zonal mean O_3 mixing ratio of the sensitivity simulations S1 and S2 (two- and fivefold CH_4, respectively) compared to the reference REF. Non-stippled areas are significant on a 95% confidence level according to a two sided Welch's test.

and eventually lead to increased O_3 abundances. Above 2 hPa, increases in OH facilitate O_3 destruction in the upper strato-sphere (Kirner et al., 2015). Beyond that, there are inter-hemispheric differences in O_3 mixing ratios in the polar regions (increased O_3 at the polar middle stratosphere at about 30 hPa) that are an indication for a strengthening of the meridional transport towards the poles in the extreme case of 5xCH_4 (see Supplement Fig. S4). In southern winter (Supple-

5 ment Fig. S4 upper right) this transport is suppressed by the polar vortex and is forming a corona of increased O_3 mixing ratios outside the polar vortex. The stratospheric cooling also leads to enhanced forming of polar stratospheric clouds (PSCs) during the southern hemispheric winter and therefore to enhanced O_3 depletion in the southern lower stratosphere (see Supplement Fig. S3 c and S4 c), (Dameris, 2010). The severity of the depletion does barely increase from S1 to S2, which may be explained by a saturation effect reached with respect of additional PSCs.

10 Overall, the twofold CH_4 mixing ratio with respect to 2010 is found to induce a radiative impact (RI) of about 0.69 Watt per square meter (W/m^2) in the twofold case (S1) and a RI of about 1.79 W/m^2 in the fivefold case (S2). The RI is calculated by the difference of the sum of long-wave and short-wave radiation at the top of the atmosphere between the reference and the respective sensitivity simulation. As the simulations are performed with prescribed SST, this net RI has the character of an effective radiative forcing (ERF), (Forster et al., 2016). It includes the RI of CH_4 itself, as well as rapid adjustments

15 from physical and chemical processes. The chemical processes specifically include changes in SWV and O_3 and have been quantified by estimating their individual RIs (including stratospheric temperature adjustments) with the EMAC submodel RAD (Dietmüller et al., 2016) in a separate simulation resulting in estimates corresponding to the reference simulation REF* and the sensitivity simulations S1* and S2* (see 2 for a detailed explanation on the simulation).

Table 1. An estimation of separate RI in [W/m^2] of the changes in the chemical species CH$_4$, SWV and O$_3$. Values are calculated using the RAD submodel (Dietmüller et al., 2016) in a separate simulation using 20 years climatologies of the individual species. Solely values of the totals are directly calculated from the presented simulations R1, S1 and S2.

Simulation	CH$_4$	SWV	O$_3$	chemical RI	physical RI[1]	total RI
S1* (2xCH4)	0.23	0.15	0.27	0.66	0.03	0.69
S2* (5xCH4)	0.51	0.55	0.76	1.82	-0.03	1.79

[1] total RI − chem. RI.

The twofolding and fivefolding CH$_4$ enhancements in the sensitivity simulations S1 and S2 correspond to a net increase of surface CH$_4$ of 1800 ppbv and 7200 ppbv, respectively. For example, the increase of the surface CH$_4$ mixing ratio from 1750 (pre-industrial) to 2011 has led to a ERF of 0.48 W/m^2±0.1 W/m^2 (IPCC, 2013, , Chap. 8, Tab. 8.2), which corresponds to a

5   net increase of surface CH$_4$ of about 1100 ppbv. The net increase of twofold CH$_4$ mixing ratios (S1) is larger than the increase since pre-industrial times. Thus, at first glance, the net RI calculated in this study seems consistent with the value in the IPCC and previous estimates from other models for a tripled CH$_4$ concentration (assumed +3534 ppbv) (Forster et al., 2016; Smith et al., 2018), which are for example for HadGEM2 1 W/m^2 and for CESM1 1.4 W/m^2.

However, those previous estimates do not account for contributions from O$_3$ and stratospheric H$_2$O changes (see also Smith

10   et al. (2018)). Only by looking at the direct RI simulations of individual species a clearer picture emerges (see Table 1). The individual RIs of the chemical variations is once more reasonable compared with similar calculations of the IPCC (Chapter 8, Figure 8.17). We detect comparably low values for the RI of CH$_4$, a feature which has been reported before for the ECHAM5 radiation module (Lohmann et al., 2010). As a residuum of the sum of chemically induced RI (Table 1) and the ERF, we estimate a pure physical RI of 0.03 W/m^2 (S1*, 2xCH$_4$) and -0.03 W/m^2 (S2*, 5xCH$_4$), respectively, i.e., small contributions

15   that compare very well to the results of Smith et al. (2018).

The separation of the individual RI in the main contributing species allows to further identify the individual contribution to temperature adjustments in the stratosphere (see Supplement Fig. S5 and S6). The stratosphere cools by about $-1 - -2$ K mostly due to SWV (up to -1.4 K). This cooling is amplified by the increased CH$_4$ and tropospheric O$_3$, but reduced by increased stratospheric O$_3$ in the area between roughly 20 hPa and 1 hPa. This induces a dipole pattern in the total temperature

20   change (warming in the lower stratosphere, cooling in the middle stratosphere, warming in the upper stratosphere and cooling in the mesosphere, see Supplement Fig. S5 and S6). Only a minor contribution to the stratospheric temperature change is contributed by tropospheric H$_2$O, as to be expected. The difference between the pure RI of all trace gas changes (Figs. S5a, S6a) and the net stratospheric temperature change (Fig. 6) is small, indicating a dominating role of radiative effects in forcing the temperature response in S1 and S2.

4 Conclusions

The present study summarizes the quasi-instantaneous chemical adjustments of the atmosphere in response to a very strong increase in atmospheric CH_4. We emphasize that the applied doubling of present day CH_4 surface mixing ratios is not unreal-
5 istic as it is even part of the RCP 8.5 scenario. Considering further feedbacks with still uncertain quantitative consequences, it is indeed possible that the presented changes in the atmospheric chemistry will be faced by upcoming generations.

For the range of CH_4 concentrations covered in this study we find that the CH_4 lifetime increases quasi-linearly with enhanced surface mixing ratios. This is ascribed to a strong reduction of OH, which is the main sink of CH_4 in the troposphere. We conclude that the strong reduction of OH will also influence other radiatively active, air quality relevant, and ozone depleting
10 substances in the troposphere. The radical OH is the most important atmospheric detergent and its reduction will enhance the residence time of these substances as well as of CH_4, and thereby increase the global radiative burden.

Additionally, induced by CH_4 oxidation, SWV will increase substantially. This leads to stratospheric cooling, which in turn influences stratospheric chemistry and (to a less degree) dynamics. In particular it will lead to an increase in total O_3 column (not shown) nearly on the whole globe. Only in the antarctic spring it causes a strengthening of the ozone depletion.
15 The rapid radiative adjustments of O_3 and SWV are both positive and thus increase the radiative forcing directly induced by CH_4, consistent with Fig. 8.17 of IPCC (2013). However, the direct CH_4 radiative impact is considerably low biased in the simulations, apparently through a systematic error in the radiation module. This bias remains masked if only the effective radiative forcing of the twofold and fivefold CH_4 simulations is considered. Individual radiative impact estimates also help interpreting the net stratospheric temperature change in the CH_4 increase simulations. It reveals that the main part of the
20 overall temperature pattern is controlled by cooling from stratospheric H_2O.

Since the SSTs are prescribed in the present simulations, tropospheric temperatures and atmospheric dynamics do not represent the situation after adaption of the ocean. This also prohibits the calculation of climate sensitivity parameters. In a future study similar CCM simulations with a mixed layer ocean will be carried out and the contribution of feedbacks associated with SST changes will be investigated accordingly.

25 *Code and data availability.* The Modular Earth Submodel System (MESSy) is continuously developed and applied by a consortium of institutions. The usage of MESSy and access to the source code is licensed to all affiliates of institutions, which are members of the MESSy Consortium. Institutions can become a member of the MESSy Consortium by signing the MESSy Memorandum of Understanding. More information can be found on the MESSy Consortium Web-site (http://www.messy-interface.org).

Author contributions. The simulations were set-up and carried out by P. J. and F. W.. F. T. analyzed the data and compiled the results. M. D.
30 and F. W. structured and composed the manuscript. M. P. and F. W. contrived and calculated the radiative impact. P. J. and M. P. contributed to the text.

Competing interests. The authors declare that they have no conflict of interest.

Acknowledgements. We acknowledge the DLR internal project KliSAW (Klimarelevanz von atmosphärischen Spurengasen, Aerosolen und Wolken), which provided the financial basis for the presented study.

5   The model simulations have been performed at the German Climate Computing Centre (DKRZ) through support from the Bundesministerium für Bildung und Forschung (BMBF).

We used the NCAR Command Language (NCL) for data analysis and to create some of the figures of this study. NCL is developed by UCAR/NCAR/CISL/TDD and available on-line: http://dx.doi.org/10.5065/D6WD3XH5.

We furthermore thank all contributors of the project ESCiMo (Earth System Chemistry integrated Modelling), which provides the model configuration and initial conditions, and Birgit Hassler for her internal review of the manuscript.

References

Braesicke, P., Keeble, J., Yang, X., Stiller, G., Kellmann, S., Abraham, N. L., Archibald, A., Telford, P., and Pyle, J. A.: Circulation anomalies in the Southern Hemisphere and ozone changes, Atmos. Chem. Phys., 13, 10 677–10 688, https://doi.org/10.5194/acp-13-10677-2013, https://www.atmos-chem-phys.net/13/10677/2013/, 2013.

Comyn-Platt, E., Hayman, G., Huntingford, C., Chadburn, S. E., Burke, E. J., Harper, A. B., Collins, W. J., Webber, C. P., Powell, T., Cox, P. M., Gedney, N., and Sitch, S.: Carbon budgets for 1.5 and 2° C targets lowered by natural wetland and permafrost feedbacks, Nature Geoscience, 11, https://doi.org/10.1038/s41561-018-0174-9, 2018.

Dalsøren, S. B., Myhre, C. L., Myhre, G., Gomez-Pelaez, A. J., Søvde, O. A., Isaksen, I. S. A., Weiss, R. F., and Harth, C. M.: Atmospheric methane evolution the last 40 years, Atmos. Chem. Phys., 16, 3099–3126, https://doi.org/10.5194/acp-16-3099-2016, https://www.atmos-chem-phys.net/16/3099/2016/, 2016.

Dameris, M.: Climate Change and Atmospheric Chemistry: How Will the Stratospheric Ozone Layer Develop?, Angewandte Chemie International Edition, 49, 8092–8102, https://doi.org/10.1002/anie.201001643, https://onlinelibrary.wiley.com/doi/abs/10.1002/anie.201001643, 2010.

Dean, J. F., J., M. J., Thomas, R., Rien, A., G., B. L., Matthias, E., M., J. M. S., E., J. A. E., H., M. O., Olivia, R., P., S. C., H., Z. M., and J., D. A.: Methane Feedbacks to the Global Climate System in a Warmer World, Reviews of Geophysics, 56, 207–250, https://agupubs.onlinelibrary.wiley.com/doi/abs/10.1002/2017RG000559, 2018.

Deckert, R. and Dameris, M.: Higher tropical SSTs strengthen the tropical upwelling via deep convection, Geophys. Res. Lett., 35, https://doi.org/10.1029/2008GL033719, https://agupubs.onlinelibrary.wiley.com/doi/abs/10.1029/2008GL033719, 2008.

Dentener, F., Peters, W., Krol, M., van Weele, M., Bergamaschi, P., and Lelieveld, J.: Interannual variability and trend of CH_4 lifetime as a measure for OH changes in the 1979–1993 time period, J. Geophys. Res., 108, 4442, https://doi.org/10.1029/2002JD002916, 2003.

Dietmüller, S., Ponater, M., and Sausen, R.: Interactive ozone induces a negative feedback in CO_2-driven climate change simulations, J. Geophys. Res. Atmos., 119, 1796–1805, https://doi.org/10.1002/2013JD020575, http://dx.doi.org/10.1002/2013JD020575, 2014.

Dietmüller, S., Jöckel, P., Tost, H., Kunze, M., Gellhorn, C., Brinkop, S., Frömming, C., Ponater, M., Steil, B., Lauer, A., and Hendricks, J.: A new radiation infrastructure for the Modular Earth Submodel System (MESSy, based on version 2.51), Geosci. Model Dev., 9, 2209–2222, https://doi.org/10.5194/gmd-9-2209-2016, https://www.geosci-model-dev.net/9/2209/2016/, 2016.

Fischer, H., Birk, M., Blom, C., Carli, B., Carlotti, M., von Clarmann, T., Delbouille, L., Dudhia, A., Ehhalt, D., Endemann, M., Flaud, J. M., Gessner, R., Kleinert, A., Koopman, R., Langen, J., López-Puertas, M., Mosner, P., Nett, H., Oelhaf, H., Perron, G., Remedios, J., Ridolfi, M., Stiller, G., and Zander, R.: MIPAS: an instrument for atmospheric and climate research, Atmos. Chem. Phys., 8, 2151–2188, https://doi.org/10.5194/acp-8-2151-2008, 2008.

Forster, P. M., Richardson, T., Maycock, A. C., Smith, C. J., Samset, B. H., Myhre, G., Andrews, T., Pincus, R., and Schulz, M.: Recommendations for diagnosing effective radiative forcing from climate models for CMIP6, J. Geophys. Res. Atmos., 121, 12 460–12 475, https://doi.org/10.1002/2016JD025320, https://agupubs.onlinelibrary.wiley.com/doi/abs/10.1002/2016JD025320, 2016.

Frank, F.: Atmospheric methane and its isotopic composition in a changing climate: A modelling study, Ph.D. thesis, Ludwigs Maximillian Universität München, 2018.

Frank, F., Jöckel, P., Gromov, S., and Dameris, M.: Investigating the yield of H_2O and H_2 from methane oxidation in the stratosphere, Atmos. Chem. Phys., 18, 9955–9973, https://doi.org/10.5194/acp-18-9955-2018, https://www.atmos-chem-phys.net/18/9955/2018/, 2018.

Garny, H.: Causes and impacts of changes in the stratospheric meridional circulation in a chemistry-climate model, Ph.D. thesis, Ludwig-Maximilians-Universität München, https://edoc.ub.uni-muenchen.de/12215/, 2010.

Garny, H., Dameris, M., Randel, W., Bodeker, G. E., and Deckert, R.: Dynamically Forced Increase of Tropical Upwelling in the Lower Stratosphere, J. Atmos. Sci., 68, 1214–1233, https://doi.org/10.1175/2011JAS3701.1, https://journals.ametsoc.org/doi/abs/10.1175/2011JAS3701.1, 2011.

Gedney, N., Cox, P. M., and Huntingford, C.: Climate feedback from wetland methane emissions, Geophys. Res. Lett., 31, https://doi.org/10.1029/2004GL020919, ttps://agupubs.onlinelibrary.wiley.com/doi/abs/10.1029/2004GL020919, 2004.

Hayes, D. J., Kicklighter, D. W., McGuire, A. D., Chen, M., Zhuang, Q., Yuan, F., Melillo, J. M., and Wullschleger, S. D.: The impacts of recent permafrost thaw on land-atmosphere greenhouse gas exchange, Environ. Res. Lett., 9, 045 005, http://stacks.iop.org/1748-9326/9/i=4/a=045005, 2014.

Hein, R., Dameris, M., Schnadt, C., Land, C., Grewe, V., Köhler, I., Ponater, M., Sausen, R., Steil, B., Landgraf, J., and Brühl, C.: Results of an interactively coupled atmospheric chemistry - general circulation model: Comparison with observations, Ann. Geophys., 19, 435–457, 2001.

Holmes, C. D.: Methane Feedback on Atmospheric Chemistry: Methods, Models, and Mechanisms, Journal of Advances in Modeling Earth Systems, 10, 1087–1099, https://doi.org/10.1002/2017MS001196, https://agupubs.onlinelibrary.wiley.com/doi/abs/10.1002/2017MS001196, 2018.

IPCC: Climate Change 2013: The Physical Science Basis. Contribution of Working Group I to the Fifth Assessment Report of the Intergovernmental Panel on Climate Change, Cambridge University Press, Cambridge, United Kingdom and New York, NY, USA, https://doi.org/10.1017/CBO9781107415324, www.climatechange2013.org, 2013.

Jöckel, P., Tost, H., Pozzer, A., Brühl, C., Buchholz, J., Ganzeveld, L., Hoor, P., Kerkweg, A., Lawrence, M. G., Sander, R., Steil, B., Stiller, G., Tanarhte, M., Taraborrelli, D., van Aardenne, J., and Lelieveld, J.: The atmospheric chemistry general circulation model ECHAM5/MESSy1: consistent simulation of ozone from the surface to the mesosphere, Atmos. Chem. Phys., 6, 5067–5104, https://doi.org/10.5194/acp-6-5067-2006, 2006.

Jöckel, P., Kerkweg, A., Pozzer, A., Sander, R., Tost, H., Riede, H., Baumgaertner, A., Gromov, S., and Kern, B.: Development cycle 2 of the Modular Earth Submodel System MESSy2, Geosci. Model Dev., 3, 717–752, https://doi.org/10.5194/gmd-3-717-2010, manual, 2010.

Jöckel, P., Tost, H., Pozzer, A., Kunze, M., Kirner, O., Brenninkmeijer, C. A. M., Brinkop, S., Cai, D. S., Dyroff, C., Eckstein, J., Frank, F., Garny, H., Gottschaldt, K.-D., Graf, P., Grewe, V., , Kerkweg, A., Kern, B., Matthes, S., Mertens, M., Meul, S., Neumaier, M., Nützel, M., Oberländer-Hayn, S., Ruhnke, R., Runde, T., Sander, R., Scharffe, D., and Zahn, A.: Earth System Chemistry integrated Modelling (ESCiMo) with the Modular Earth Submodel System (MESSy) version 2.51, Geosci. Model Dev., 9, 1153–1200, https://doi.org/10.5194/gmd-9-1153-2016, http://www.geosci-model-dev.net/9/1153/2016/gmd-9-1153-2016.html, 2016.

Karlsdóttir, S. and Isaksen, I. S. A.: Changing methane lifetime: Possible cause for reduced growth, Geophys. Res. Lett., 27, 93–96, https://doi.org/10.1029/1999GL010860, http://dx.doi.org/10.1029/1999GL010860, 2000.

Kirner, O., Ruhnke, R., and Sinnhuber, B.-M.: Chemistry–Climate Interactions of Stratospheric and Mesospheric Ozone in EMAC Long-Term Simulations with Different Boundary Conditions for CO_2, CH_4, N_2O, and ODS, Atmosphere-Ocean, 53, 140–152, https://doi.org/10.1080/07055900.2014.980718, 2015.

Klappenbach, F., Bertleff, M., Kostinek, J., Hase, F., Blumenstock, T., Agusti-Panareda, A., Razinger, M., and Butz, A.: Accurate mobile remote sensing of XCO_2 and XCH_4 latitudinal transects from aboard a research vessel, Atmos. Meas. Tech., 8, 5023–5038, https://doi.org/10.5194/amt-8-5023-2015, https://www.atmos-meas-tech.net/8/5023/2015/, 2015.

Koven, C. D., Lawrence, D. M., and Riley, W. J.: Permafrost carbon-climate feedback is sensitive to deep soil carbon decomposability but not deep soil nitrogen dynamics, Proceedings of the National Academy of Sciences, 112, 3752–3757, https://doi.org/10.1073/pnas.1415123112, http://www.pnas.org/content/112/12/3752, 2015.

5 Lohmann, U., Rotstayn, L., Storelvmo, T., Jones, A., Menon, S., Quaas, J., Ekman, A. M. L., Koch, D., and Ruedy, R.: Total aerosol effect: radiative forcing or radiative flux perturbation?, Atmos. Chem. Phys., 10, 3235–3246, https://doi.org/10.5194/acp-10-3235-2010, https://www.atmos-chem-phys.net/10/3235/2010/, 2010.

Ma, S., Jiang, J., Huang, Y., Shi, Z., Wilson, R. M., Ricciuto, D., Sebestyen, S. D., Hanson, P. J., and Luo, Y.: Data-Constrained Projections of Methane Fluxes in a Northern Minnesota Peatland in Response to Elevated CO2 and Warming, J. Geophys. Res. Biogeosci., 122,

10 2841–2861, https://doi.org/10.1002/2017JG003932, https://agupubs.onlinelibrary.wiley.com/doi/pdf/10.1002/2017JG003932, 2017.

MacKay, R. and Khalil, M.: Theory and development of a one dimensional time dependent radiative convective climate model, Chemosphere, 22, 383–417, https://doi.org/10.1016/0045-6535(91)90326-9, http://www.sciencedirect.com/science/article/pii/0045653591903269, 1991.

Miller, S. M., Taylor, M. A., and Watts, J. D.: Understanding high-latitude methane in a warming climate, Eos (Earth & Space Science News), 99, https://doi.org/10.1029/2018EO091947, 2018.

15 Montzka, S. A., Krol, M., Dlugokencky, E., Hall, B., Lelieveld, P. J., and Jöckel, P.: Small Interannual Variability of Global Atmospheric Hydroxyl, Science, 331, 67–69, 2011.

Naik, V., Voulgarakis, A., Fiore, A. M., Horowitz, L. W., Lamarque, J.-F., Lin, M., Prather, M. J., Young, P. J., Bergmann, D., Cameron-Smith, P. J., Cionni, I., Collins, W. J., Dalsøren, S. B., Doherty, R., Eyring, V., Faluvegi, G., Folberth, G. A., Josse, B., Lee, Y. H., MacKenzie, I. A., Nagashima, T., van Noije, T. P. C., Plummer, D. A., Righi, M., Rumbold, S. T., Skeie, R., Shindell, D. T., Stevenson,

20 D. S., Strode, S., Sudo, K., Szopa, S., and Zeng, G.: Preindustrial to present-day changes in tropospheric hydroxyl radical and methane lifetime from the Atmospheric Chemistry and Climate Model Intercomparison Project (ACCMIP), Atmos. Chem. Phys., 13, 5277–5298, https://doi.org/10.5194/acp-13-5277-2013, https://www.atmos-chem-phys.net/13/5277/2013/, 2013.

O'Connor, F. M., Boucher, O., Gedney, N., Jones, C. D., Folberth, G. A., Coppell, R., Friedlingstein, P., Collins, W. J., Chappellaz, J., Ridley, J., and Johnson, C. E.: Possible role of wetlands, permafrost, and methane hydrates in the methane cycle under future climate change: A

25 review, Rev. Geophys., 48, https://doi.org/10.1029/2010RG000326, rG4005, 2010.

Owens, A. J., Steed, J. M., Filkin, D. L., Miller, C., and Jesson, J. P.: The Potential effects of increased methane on atmospheric ozone, Geophys. Res. Lett., 9, 1105–1108, https://doi.org/10.1029/GL009i009p01105, http://dx.doi.org/10.1029/GL009i009p01105, 1982.

Plieninger, J. F.: Ableitung von CH$_4$ und N$_2$O aus MIPAS - ENVISAT-Beobachtungen, Ph.D. thesis, Karlsruher Institut für Technologie Fakultät Physik, 2017.

30 Portmann, R. W. and Solomon, S.: Indirect radiative forcing of the ozone layer during the 21st century, Geophys. Res. Lett., 34, https://doi.org/10.1029/2006GL028252, https://agupubs.onlinelibrary.wiley.com/doi/abs/10.1029/2006GL028252, 2007.

Rayner, N. A., Parker, D. E., Horton, E. B., Folland, C. K., Alexander, L. V., Rowell, D. P., Kent, E. C., and Kaplan, A.: Global analyses of sea surface temperature, sea ice, and night marine air temperature since the late nineteenth century, J. Geophys. Res. Atmos., 108, https://doi.org/10.1029/2002JD002670, 4407, 2003.

35 Revell, L., Stenke, A., Rozanov, E., Ball, W., Lossow, S., and Peter, T.: The role of methane in projections of 21st century stratospheric water vapour, Atmos. Chem. Phys., 16, 13067–13080, https://doi.org/10.5194/acp-16-13067-2016, www.atmos-chem-phys.net/16/13067/2016/, 2016.

Riahi, K., Grübler, A., and Nakicenovic, N.: Scenarios of long-term socio-economic and environmental development under climate stabilization, Technological Forecasting and Social Change, 74, 887–935, https://doi.org/10.1016/j.techfore.2006.05.026, http://www.sciencedirect.com/science/article/pii/S0040162506001387, 2007.

5 Riahi, K., Rao, S., Krey, V., Cho, C., Chirkov, V., Fischer, G., Kindermann, G., Nakicenovic, N., and Rafaj, P.: RCP 8.5—A scenario of comparatively high greenhouse gas emissions, Climatic Change, 109, 33, https://doi.org/10.1007/s10584-011-0149-y, 2011.

Röckmann, T., Brass, M., Borchers, R., and Engel, A.: The isotopic composition of methane in the stratosphere: high-altitude balloon sample measurements, Atmos. Chem. Phys., 11, 13 287–13 304, https://doi.org/10.5194/acp-11-13287-2011, 2011.

Rohs, S., Schiller, C., Riese, M., Engel, A., Schmidt, U., Wetter, T., Levin, I., Nakazawa, T., and Aoki, S.: Long-term changes of methane
10 and hydrogen in the stratosphere in the period 1978-2003 and their impact on the abundance of stratospheric water vapor, J. Geophys. Res. Atmos., 111, 1–12, https://doi.org/10.1029/2005JD006877, 2006.

Saunois, M., Jackson, R. B., Bousquet, P., Poulter, B., and Canadell, J. G.: The growing role of methane in anthropogenic climate change, Environ. Res. Lett., 11, 120 207, http://stacks.iop.org/1748-9326/11/i=12/a=120207, 2016.

Schaefer, K., Lantuit, H., Romanovsky, V. E., Schuur, E. A. G., and Witt, R.: The impact of the permafrost carbon feedback on global climate,
15 Environ. Res. Lett., 9, 085 003, http://stacks.iop.org/1748-9326/9/i=8/a=085003, 2014.

Schuur, E. A. G., McGuire, A. D., Schädel, C., Grosse, G., Harden, J. W., Hayes, D. J., Hugelius, G., Koven, C. D., Kuhry, P., Lawrence, D. M., Natali, S. M., Olefeldt, D., Romanovsky, V. E., Schaefer, K., Turetsky, M. R., Treat, C. C., and Vonk, J. E.: Climate change and the permafrost carbon feedback, Nature, 520, 171–179, https://doi.org/10.1038/nature14338, 2015.

Shang, L., Liu, Y., Tian, W., and Zhang, Y.: Effect of methane emission increases in East Asia on atmospheric circulation and ozone, Advances
20 in Atmospheric Sciences, 32, 1617–1627, https://doi.org/10.1007/s00376-015-5028-4, https://doi.org/10.1007/s00376-015-5028-4, 2015.

Smith, C. J., Kramer, R. J., Myhre, G., Forster, P. M., Soden, B., Andrews, T., Boucher, O., Faluvegi, G., Fläschner, D., Hodnebrog, O. ., Kasoar, M., Kharin, V., Kirkevå g, A., Lamarque, J.-F., Mülmenstädt, J., Olivié, D., Richardson, T., Samset, B. H., Shindell, D., Stier, P., Takemura, T., Voulgarakis, A., and Watson-Parris, D.: Understanding Rapid Adjustments to Diverse Forcing Agents, Geophysical Research Letters, 0, https://doi.org/10.1029/2018GL079826, https://agupubs.onlinelibrary.wiley.com/doi/abs/10.1029/2018GL079826, 2018.

25 Stenke, A. and Grewe, V.: Simulation of stratospheric water vapor trends: impact on stratospheric ozone chemistry, Atmos. Chem. Phys., 5, 1257–1272, www.atmos-chem-phys.org/acp/5/1257/, 2005.

Voulgarakis, A., Naik, V., Lamarque, J.-F., andP. J. Young, D. T. S., Prather, M. J., Wild, O., Field, R. D., andP. Cameron-Smith, D. B., Cionni, I., Collins, W. J., andR. M. Doherty, S. B. D., Eyring, V., Faluvegi, G., Folberth, G. A., Horowitz, L. W., Josse, B., MacKenzie, I. A., Nagashima, T., Plummer, D. A., Righi, M., Rumbold, S. T., Stevenson, D. S., Strode, S. A., Sudo, K., Szopa, S., and Zeng,
30 G.: Analysis of present day and future OH and methane lifetime in the ACCMIP simulations, Atmos. Chem. Phys., 13, 2563–2587, https://doi.org/10.5194/acp-13-2563-2013, 2013.

Zhang, Z., Zimmermann, N. E., Stenke, A., Li, X., Hodson, E. L., Zhu, G., Huang, C., and Poulter, B.: Emerging role of wetland methane emissions in driving 21st century climate change, Proceedings of the National Academy of Sciences, 114, 9647–9652, https://doi.org/10.1073/pnas.1618765114, http://www.pnas.org/content/114/36/9647, 2017.

<